JOURNAL OF THERMOPHYSICS AND HEAT TRANSFER
Vol. 6, No. 4, Oct.–Dec. 1992

Investigation of Liquid Droplet Evaporation in Subcritical and Supercritical Gaseous Environments

H. Jia* and G. Gogos†
Rutgers University, Piscataway, New Jersey 08855

Droplet vaporization in a high-pressure and temperature stagnant environment has been investigated numerically. Results are presented for a *n*-hexane droplet evaporating into nitrogen, for ambient pressures of 1–100 atm and temperatures of 500–1250 K. The high-pressure model accounts for 1) transients in both the liquid and the gas phase; 2) real gas effects in calculating the gas phase density, the energy required for phase change, and the droplet surface vapor-liquid equilibrium composition; and 3) it accounts for gas phase transport and thermodynamic properties varying with temperature, pressure, and composition. The droplet lifetime dependence on ambient pressure and temperature has been predicted. At the lowest ambient temperature considered (500 K), the droplet lifetime increases monotonically with ambient pressure, at least for the pressure range investigated. At a higher ambient temperature of 600 K, it exhibits a maximum with ambient pressure. At an ambient temperature of 1000 K, the droplet lifetime is less sensitive to pressure. At even higher ambient temperatures (1250 K), it decreases monotonically with pressure. The steady-state vaporization assumption underpredicts droplet lifetimes substantially with increasing ambient pressure.

I. Introduction and Literature Review

THE understanding of droplet vaporization at high pressure and temperature environments is of importance to many industrial applications such as liquid-fueled rocket engines and diesel engines. During spray combustion in such devices, droplets frequently evaporate in the relatively cool interior of the spray.[1] The vaporization process may occur at pressures near or above the critical pressure of the fuel. Therefore, many effects that are assumed negligible at low and moderate ambient pressure need to be re-evaluated. Among these effects are, the transient character of the gas phase, nonideal gas phase behavior, the real gas effect on the heat of vaporization, and the vapor-liquid equilibrium condition at the droplet interface. Considering these effects, we have formulated a high-pressure model for droplet vaporization. Results using this model have been obtained numerically.

Many fundamental studies concerning both experimental and theoretical research on evaporation of a single droplet at atmospheric or near atmospheric pressures are available in the literature. There are many excellent and authoritative reviews on the subject.[1–4] However, studies on droplet vaporization at elevated ambient pressures are more scarce. In the next few paragraphs we present a review of these studies.

Matlosz et al.[5] conducted an experimental investigation of the evaporation of a *n*-hexane droplet at subcritical and supercritical environment. A gas environment that has a temperature and pressure greater than the critical temperature and pressure of the liquid was defined as supercritical environment. The drop was suspended from a fine wire thermocouple and vaporized into a nitrogen or argon environment. The ambient temperature was 548 K, and pressures ranged from 6.8 to 102 atm (the critical temperature and pressure of *n*-hexane are 507.4 K and 29.3 atm, respectively). Droplet diameters ranged between 770–1780 μm. Their experimental results showed that droplet lifetime decreased with increasing ambient pressure.

Manrique and Borman[6] conducted a numerical study on steady-state vaporization for liquid carbon dioxide droplets at high ambient pressures. By steady state, it was implied that all the energy arriving at the droplet surface was utilized for vaporization, while the droplet remained at a constant temperature. Their model considered nonideal gas effects, variable properties, and solubility of the inert gas in the liquid phase. Results were reported for ambient temperatures of 500–1600 K and pressures of 70–120 atm. The authors predicted that steady-state mass vaporization rate increased with increasing ambient pressure and/or increasing ambient temperature. This means that for steady-state vaporization, the droplet lifetime would decrease with increasing ambient pressure.

Hubbard et al.[7] presented a numerical model of single droplet evaporation that included transient gas and liquid phases, gas phase variable properties, and ideal gas law. They presented results for a *n*-octane droplet evaporating in air at moderate environment pressures (1, 5, and 10 atm), with droplet diameters from 20 to 500 μm, initial temperature of 300 K, and ambient temperatures of 600–2000 K. Their results showed that for the pressure range considered, the droplet lifetime increased with increasing pressure.

Curtis and Farrell[8] and Curtis et al.[9] developed a numerical model for droplet vaporization in an environment above the liquid critical pressure, and near, or above, the liquid critical temperature. The authors predicted droplet size histories, surface temperature histories, liquid and gas phase temperature profiles, and mass fraction profiles of vaporizing species in the gas field for *n*-octane droplets.

Hsieh et al.[10] investigated numerically multicomponent droplet vaporization at near critical conditions. The influence of transient effects, surface regression, ambient gas solubility, and phase-equilibrium relations on vaporization mechanisms were examined in detail.

In a more recent study Delplanque and Sirignano[11] developed an elaborate numerical model (of moderate complexity, so that it can be used in a larger spray combustion code) to investigate burning of an oxygen droplet at sub- and near-critical conditions. Their paper also includes computations on the vaporization of an oxygen droplet in hydrogen at elevated ambient pressures. It was shown that unsteady effects in the gas phase are very important. Under supercritical pressures, the droplet surface temperature reaches the computed critical mixture value.

Received May 30, 1991; revision received Nov. 12, 1991; accepted for publication Nov. 15, 1991.

*Graduate Student, Department of Mechanical and Aerospace Engineering, P.O. Box 909.

†Assistant Professor, Department of Mechanical and Aerospace Engineering, P.O. Box 909. Member AIAA.

The above review reveals that the droplet lifetime dependence on ambient pressure has not been resolved. The numerical investigation of Hubbard et al.[7] is limited to a short range of low-ambient pressures (1–10 atm), and predicts that the droplet lifetime may increase with ambient pressure. The experimental study of Matlosz et al.,[5] however, that was conducted over a wide range of high ambient pressures (6.8–102 atm) and a single ambient temperature of 548 K, predicts a monotonic decrease of droplet lifetime with ambient pressure. This experimental study was conducted with large droplets (0.77–1.78 mm in diameter), under the influence of natural convection. Due to the large size and the high-pressure environment, buoyancy effects should have been very important in this experiment. Furthermore, natural convection effects become more important with increasing pressure. This probably leads to the monotonic decrease of droplet lifetime with increasing pressure, predicted in the above mentioned study. Finally, the numerical investigation of Manrique and Borman[6] was conducted under the steady-state assumption; heat-up of the droplet interior was neglected, and the gas phase was treated as quasisteady. This is a severe assumption because 1) the heat-up of the droplet becomes more important with increasing pressure since the wet bulb temperature increases with pressure[1]; and 2) the gas phase quasisteadiness breaks down with increasing pressure, because the gas-to-liquid phase density ratio does not remain small compared to unity at high pressures. The purpose of our investigation is to develop an elaborate numerical model for spherically symmetric droplet vaporization, that among other quantities of interest, will be able to predict and explain droplet lifetime behavior for a wide range of ambient pressures and temperatures. The literature related to the problem of high-pressure droplet combustion is more extensive,[11–20] and will not be reviewed here.

Finally, while the present work was under review, an article by Hsieh et al.,[21] employing a similar model, appeared in the literature. Although the models developed in both articles are similar, the two studies differ in several important aspects. The present article contains additional results, and improves significantly, upon some results presented in Ref. 21. Actually, the focus of the present study, namely, prediction of droplet lifetime behavior for a wide range of ambient pressures and temperatures, has not been addressed adequately in Ref. 21. Hsieh et al.[21] limited their results to a single ambient temperature of 2000 K, and predicted that the droplet evaporation rate increases progressively with pressure. Figure 8 of the present article provides an exhaustive presentation of the droplet lifetime dependence on ambient pressure for different ambient temperatures. Thus, plotted vs ambient pressure 1) the droplet lifetime increases monotonically at low ambient temperatures (500 K); 2) presents a maximum for higher ambient temperatures (600 K); 3) becomes insensitive to pressure at a temperature of 1000 K; and 4) only at much higher temperatures (1250 K) does it start exhibiting the dependence predicted by Hsieh et al.[21] The range of temperatures considered in the present work (500–1250 K) are of practical interest. Temperature measurements available in the literature[1,22–26] show that the center of the spray is cool, making the above temperature range of particular importance. Additional significant results that distinguish the present article are presented in Figs. 9 and 10. In Fig. 9, it is shown that the steady-state assumption, as employed by Manrique and Borman,[6] breaks down at elevated pressures, and underpredicts droplet lifetimes substantially with increasing ambient pressure. The importance of droplet heat-up, as compared to droplet lifetime at high ambient pressures, is clearly shown in Fig. 10.

The ultimate goal in our research effort on high-pressure droplet vaporization is to eventually develop a numerical model that will include natural convection effects. In the present study, however, we are considering spherically symmetric vaporization. The various high-pressure effects that need to be included in a comprehensive model (nonideal gas phase behavior, real gas effect on heat of vaporization, real gas effect on vapor-liquid equilibrium condition at the droplet interface, variable transport and thermodynamic properties, and transient character of both liquid and gas phases) render the problem adequately challenging. In addition to being a first step in our research effort, spherically symmetric vaporization in supercritical conditions is of practical interest for microgravity environments. The theoretical formulation for a droplet vaporizing in a high-pressure and temperature stagnant environment is provided in the next section.

II. Problem Formulation

Consider a single component liquid droplet of initial radius R_0 evaporating into a stagnant inert environment of infinite expanse. The initial temperature of the droplet is T_0 and the ambient pressure and temperature are P_∞ and T_∞, respectively.

As discussed earlier, gravitational effects are neglected, and the only convective motion considered is that induced by vaporization. This causes a radial flowfield in the gas phase. In the analysis that follows, subscripts 1 and 2 refer to the vaporizing species and the inert gas present in the stagnant environment, respectively.

The main features (to be discussed in more detail later in this section) of the high pressure numerical model are as follows:

1. Both gas and liquid phase processes are considered transient. The gas phase quasisteady assumption is valid when the gas-to-liquid phase density ratio is much less than unity ($\rho/\rho l \ll 1$). At high enough pressure this assumption is not valid. For the same reason, regression motion of the droplet surface is taken into consideration in the model.

2. To capture the real gas behavior of the gas phase at high pressures, the modified Redlich-Kwong equation of state developed by Chueh and Prausnitz[27] is employed. This is one of the most highly employed[5,6,8,9–11,15,17] and most successful two parameter equations of state.

3. The mole fraction of the vaporizing species at the droplet surface is calculated by assuming thermodynamic equilibrium. At low pressures the following assumptions are usually employed: 1) the gas phase mixture obeys the equation of state for ideal gases and Dalton's law; and 2) the inert gas present in the mixture does not affect the equilibrium vapor pressure of pure species 1 at the droplet surface temperature. With these assumptions, the mole fraction of the vaporizing species at the droplet surface is given by $y_1 = P_1/P$, where y_1 is the mole fraction of the vaporizing species, P_1 is the vapor pressure of pure component 1 at the droplet surface temperature, and P is the total ambient pressure. In the present study, however, both assumptions are invalid due to the high pressure. The composition of the real gas mixture at the droplet surface is provided by the equilibrium condition that the fugacity of each species at the liquid phase is equal to the fugacity of the same species in the gas phase.

4. With low-pressure models, the latent heat of vaporization of pure species 1, at the droplet surface temperature, is taken as the energy required for phase change. At high pressures, however, as shown by Manrique and Borman,[6] real gas effects play an important role on the energy required for phase change and are included in the present model.

5. The gas phase transport and thermodynamic properties are considered varying with temperature, composition, and pressure. The liquid phase properties are evaluated at a reference temperature.

The following assumptions are employed: 1) the pressure is constant, for spherically symmetric vaporization, the radial momentum equation is usually ignored[1,4,11]; 2) solubility of inert gas in the liquid phase is neglected, this assumption imposes upper limits on the ambient pressures and temperatures that can be considered in this study, and will be discussed in detail in a later section; 3) the droplet shape remains spherical; 4) radiation is negligible; 5) second order effects

such as the Soret and Dufour effects are negligible; and 6) viscous dissipation is neglected.

The governing conservation equations in spherical coordinates are:

For the gaseous phase, $r > R(t)$

Continuity Equation

$$\frac{\partial \rho}{\partial t} + \frac{1}{r^2}\frac{\partial}{\partial r}(\rho r^2 v_r) = 0 \tag{1}$$

Species Equation

$$\frac{\partial m_1}{\partial t} + v_r \frac{\partial m_1}{\partial r} = \frac{1}{\rho r^2}\frac{\partial}{\partial r}\left(\rho D_{12} r^2 \frac{\partial m_1}{\partial r}\right) \tag{2}$$

Energy Equation

$$\frac{\partial T}{\partial t} + v_r \frac{\partial T}{\partial r} = \frac{1}{\rho r^2}\frac{\partial}{\partial r}\left(\frac{k}{c_p} r^2 \frac{\partial T}{\partial r}\right) + \frac{D_{12}}{c_p}\frac{\partial T}{\partial r}\left[(c_{p1} - c_{p2})\frac{\partial m_1}{\partial r} + Le \frac{\partial c_p}{\partial r}\right] \tag{3}$$

In the above equations, t and r refer to temporal and spatial variables, R is the instantaneous radius of the droplet, T is the temperature, ρ, k, and c_p are the density, thermal conductivity, and specific heat at constant pressure of the gaseous mixture; v_r is the radial velocity induced by vaporization, m_1 is the fuel vapor mass fraction, D_{12} is the binary mass diffusion coefficient, and c_{p1} and c_{p2} are the specific heats at constant pressure for pure species 1 and 2. $Le = k/\rho D_{12} c_p$ is the Lewis number.

For the liquid phase, $r < R(t)$

Energy Equation

$$\frac{\partial T}{\partial t} = \frac{\alpha_l}{r^2}\frac{\partial}{\partial r}\left(r^2 \frac{\partial T}{\partial r}\right) \tag{4}$$

where subscript l indicates liquid phase and α_l is the thermal diffusivity of the liquid. The boundary conditions are:

At the droplet center

$$\frac{\partial T}{\partial r} = 0 \tag{5}$$

As $r \to \infty$

$$T \to T_\infty \tag{6}$$

$$m_1 \to m_{1,\infty} \tag{7}$$

$$v_r \to 0 \tag{8}$$

At the droplet surface

Mass Conservation

$$v_r = \dot{m}''[(1/\rho) - (1/\rho_l)] \tag{9}$$

Impermeability Condition

$$(1 - m_1)\dot{m}'' = -\rho D_{12}\frac{\partial m_1}{\partial r} \tag{10}$$

Temperature Continuity

$$T_g = T_l \tag{11}$$

Heat Flux Continuity

$$k\left.\frac{\partial T}{\partial r}\right|_g = k_l \left.\frac{\partial T}{\partial r}\right|_l + \dot{m}''\Delta h \tag{12}$$

Vapor-Liquid Equilibrium Relationship

$$m_1 = m_1(T_s, P) \tag{13}$$

The overall mass-conservation condition that determines the rate of change of the droplet radius is given by

$$\frac{dR}{dt} = -\frac{\dot{m}''}{\rho_l} \tag{14}$$

In the above equations $\dot{m}''$ is the mass flux at the droplet surface, subscripts g and s indicate gas phase and droplet surface, respectively, and Δh is the energy required for change of phase.

In addition to the above equations, an equation of state that accounts for the behavior of real gases is needed. The modified Redlich-Kwong equation developed by Chueh and Prausnitz[27] has been employed, and is given in the form

$$P = [(R_u T)/(v - b)] - [a/T^{0.5} v(v + b)] \tag{15}$$

where v is the specific volume of the gaseous mixture, R_u is the universal gas constant, and a and b are the two parameters. The parameters a and b, which are constant for pure compounds, are made composition dependent through the mixing rules proposed by Chueh and Prausnitz.[27] It can easily be shown that Eq. (15) is a cubic polynomial in v. Its largest real root provides the specific volume v of the gaseous mixture.

In the next few paragraphs, the vapor-liquid equilibrium relationship, the energy required for change of phase, and the transport and thermodynamic properties are discussed.

For thermodynamic equilibrium, in addition to the temperature and pressure being equal, the fugacity of each component must be the same in both phases, namely

$$f_i^v = f_i^l \tag{16}$$

where superscripts v and l indicate vapor and liquid phase, respectively. Using Eq. (16) it may be shown that in view of assumption 2, the vapor-liquid equilibrium relationship, Eq. (13), takes the form[5]

$$y_1(P, T) = \frac{P_{vp,1}(T)}{P}\frac{\phi_1^{\text{sat}}(T)}{\phi_1}\exp\left(\int_{P_{vp,1}}^{P}\frac{v_1^l(T, P)}{R_u T}\,dP\right) \tag{17}$$

where $P_{vp,1}$ is saturated pressure of pure fuel vapor at temperature T, v_1^l is its liquid molar volume, ϕ_1^{sat} is fugacity coefficient at saturated conditions given by $f_1^{v,\text{sat}}/P_{vp,1}$ and ϕ_1 is the fugacity coefficient of the vapor and is given by $f_1^v/y_1 P$. Both $P_{vp,1}$ and ϕ_1^{sat} are functions of temperature only. The liquid molar volume weakly changes with pressure, and is approximated by the molar volume of the saturated liquid at the same temperature, namely, $v^l(P, T) \simeq v^l(T)$. The fugacity coefficient, ϕ_1, is a function of pressure, temperature, and gas composition. The following thermodynamic relation provides ϕ_1 in terms of the volumetric properties of the mixture:

$$R_u T \ln \phi_1 = \int_v^\infty \left[\left(\frac{\partial P}{\partial n_1}\right)_{T,v,n_2} - \frac{R_u T}{v}\right] dv - R_u T \ln z \tag{18}$$

where z is the compressibility factor and n_i is the number of moles of the ith species. By substituting the Redlich-Kwong equation with the mixing rules proposed by Cheuh and

Prausnitz[27] the fugacity of the ith component in the gaseous mixture is given by

$$\ln \phi_i = \ln \frac{v}{v-b} + \frac{b_i}{v-b} - \left(2\sum_{j=1}^{N} y_j a_{ij}\right)\Big/(R_u T^{3/2} b) \cdot \ln \frac{v+b}{v} + \frac{ab_i}{R_u T^{3/2} b^2}\left(\ln \frac{v+b}{v} - \frac{b}{v+b}\right) - \ln \frac{Pv}{R_u T} \tag{19}$$

Deviation between the usually assumed latent heat of vaporization for pure component, and the enthalpy required for vaporization into a gas mixture, is determined by employing the Redlich-Kwong equation of state. The energy required for phase change, Δh, is given by

$$\Delta h = \tilde{H}_1(T, P, y_i) - H_l(T, P) \tag{20}$$

where $\tilde{H}_1$ is the partial enthalpy of the vaporizing component at a given temperature, pressure, and composition, and H_l is its molar enthalpy in the liquid phase at the same pressure and temperature. The partial enthalpy $\tilde{H}_1$ of component 1 and its ideal gas enthalpy H_1^0 at the same temperature are related through the thermodynamic relation

$$-\Delta H_1 = (H_1^0 - \tilde{H}_1)_T = R_u T^2 \left(\frac{\partial \ln \phi_1}{\partial T}\right)_{P,y} \tag{21}$$

where ΔH_1 is the deviation between the ideal gas enthalpy and partial enthalpy. Subscript y in Eq. (21) indicates differentiation at constant composition. Substituting Eq. (21) into Eq. (20) we obtain

$$\Delta h = H_1^0(T) - H_l(T, P) + \Delta H_1 \tag{22}$$

where low pressure enthalpy is given by

$$H_1^0(T) = \int_{T_0}^{T} c_{p1}^0 \, dT \tag{23}$$

and c_{p1}^0 is the specific heat at constant pressure for ideal gas.

The heat capacity at constant pressure of a real gas is given by

$$c_p = \sum_{i=1}^{N} y_i c_{pi}^0 + \Delta c_p \tag{24}$$

where superscript 0 indicates ideal gas and the residual heat capacity, Δc_p, is obtained using the Redlich-Kwong equation of state as recommended by Reid et al.[28]

The binary mass diffusion coefficient D_{12} is calculated based on the theory of Chapman and Enskog, with collision integral given in Ref. 29. The Roy and Thodos estimation technique[30] is used for thermal conductivity of hydrocarbons and the modified Eucken method[28] for nonhydrocarbons. Wilke's rule is then utilized to calculate k for mixtures. Finally, equations by Reid et al.[28] are used to correct for high-pressure effects on the above transport properties. More specifically, the Stiel and Thodos correlation[31] with the Prausnitz and Gunn rules[32] for the pseudocritical properties is used for k, and the Takahashi correlation[33] for D_{12}.

III. Method of Solutions

Solutions to the model are pursued in a spatial coordinate system which is described as follows:

For liquid phase

$$r^* = (r/R) \tag{25}$$

For gaseous phase

$$r^{**} = \ln (r/R) \tag{26}$$

where $0 \le r^* \le 1$ and $0 \le r^{**} < \infty$. In view of Eq. (26), using a constant step size Δr^{**}, grid points in the gaseous phase are clustered close to the droplet interface where gradients are steep. Furthermore, the gas-phase outer boundary in the physical domain can be kept far away from the droplet surface with a small number of grid points leading to efficient computing.

The fully implicit scheme (backward-time, central-space) was utilized to discretize the governing equations and boundary conditions.[34] The procedure for calculating one time step is given as follows: properties of gaseous phase are calculated at the temperature, pressure, and composition from previous time step. Then T, m_1, v_r, and $\dot{m}''$ are solved iteratively using Eqs. (1)–(12), together with Eq. (17) until the following condition is satisfied:

$$\left|1 - \frac{\dot{m}''^0}{\dot{m}''}\right| < \varepsilon \tag{27}$$

where superscript 0 indicates previous iteration. In the above iterative calculations, density is obtained from the Redlich-Kwong equation, velocity is obtained by integrating Eq. (1) by the Euler predictor-corrector method and $\varepsilon = 10^{-5}$. The radial velocity at the droplet surface is given by Eq. (9) and droplet radius is updated using Eq. (14).

For the gas phase, exponential profiles for temperature and mass fraction of vapor and velocity decaying as $1/r^2$ were assumed as initial conditions. Through numerical experimentation, it was found that the shapes of the initial profiles affect the results negligibly. Solutions invariant with step size were obtained by halfing the step size. Thus, $\Delta r^* = \Delta r^{**} = 0.01$, and Δt approximately $\frac{1}{250}$ of the droplet lifetime were found to be adequately small for the computations. Calculations were terminated when $(R/R_0)^2 < 0.2$.

IV. Results and Discussion

Results for a n-hexane droplet evaporating into a nitrogen environment will be presented in Sec. IV.B. Before presenting these results, several key aspects of our model are discussed in Sec. IV.A. This discussion is helpful in understanding the global results of droplet vaporization, presented in Sec. IV.B.

A. Further Discussion of the Model

In this section, a n-hexane-nitrogen system in thermodynamic equilibrium is discussed. Figure 1 shows the mole fraction of n-hexane, either calculated by Eq. (17), or measured by Poston and McKetta,[35] as a function of total pressure for a n-hexane-nitrogen equilibrium system at four different isotherms (344.3, 377.6, 410.9, and 444.3 K). There is a good agreement between the calculated and the experimentally obtained values.

For isotherms close to the critical temperature of n-hexane, or for very high total pressures, the theory fails to predict equilibrium mole fraction. This problem was also encountered by Matlosz et al.[5] and places an upper limit on the total pressures that can be considered. The fact that equilibrium is assumed to exist only for the vaporizing species, whereas the inert species is present only in the gas phase, was provided as the reason for this difficulty. Fig. 2 presents this limit. The domain to the left of the curve provides the region where equilibrium mole fraction can be predicted. Implementation of this limit will become clear in Sec. IV.B.

Figure 3 shows the energy required for phase change for a n-hexane-nitrogen system in equilibrium. Equation (22) is utilized in predicting the real gas effect. As the total pressure increases, the deviation between the latent heat for pure species and the energy required for the binary system becomes significant. The energy required for vaporization for a binary

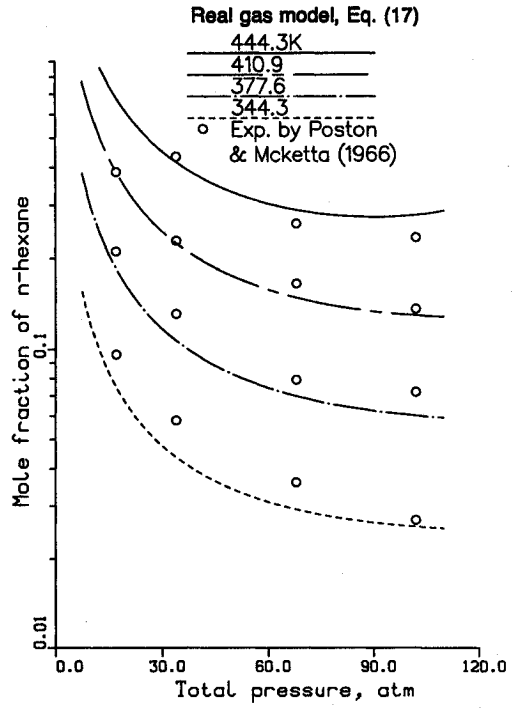

Fig. 1 Equilibrium mole fraction of *n*-hexane in the gas phase as a function of total pressure at four different isotherms for a *n*-hexane-nitrogen system.

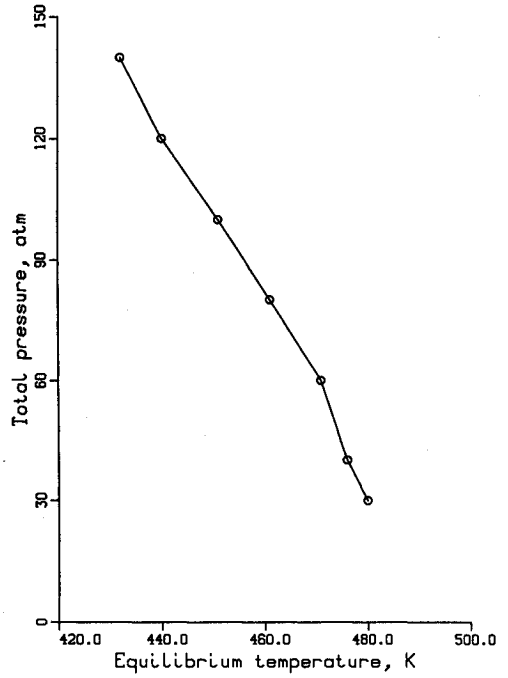

Fig. 2 Limitation on pressure-temperature conditions for which equilibrium mole fractions can be predicted for a *n*-hexane-nitrogen system.

system decreases with increasing pressure and temperature. The temperature increase near the critical temperature of *n*-hexane causes an abrupt decrease of the energy required for phase change for the binary system, as for the latent heat of vaporization for pure species.

B. Results

Results will be presented for a *n*-hexane droplet evaporating into a nitrogen environment ($m_{1,\infty} = 0$) with initial size $R_0 = 2.5 \times 10^{-4}\ m$, and initial temperature $T_0 = 300$ K.

Figures 4 and 5 show the temporal variation of the droplet surface temperature. At low and moderate ambient pressures,

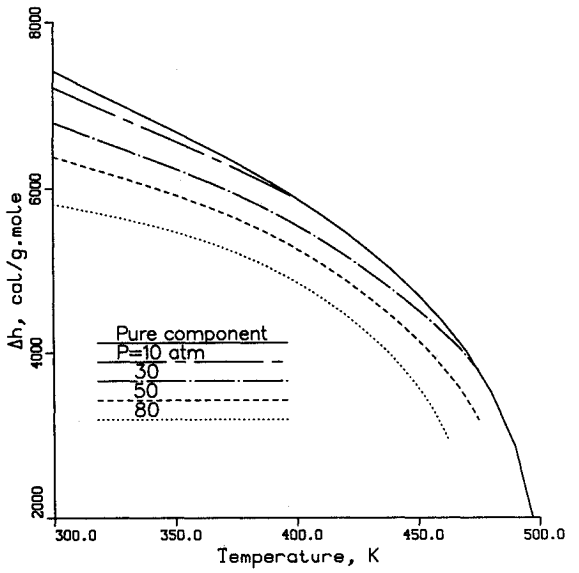

Fig. 3 Real gas effect on energy required for phase change for a *n*-hexane-nitrogen system.

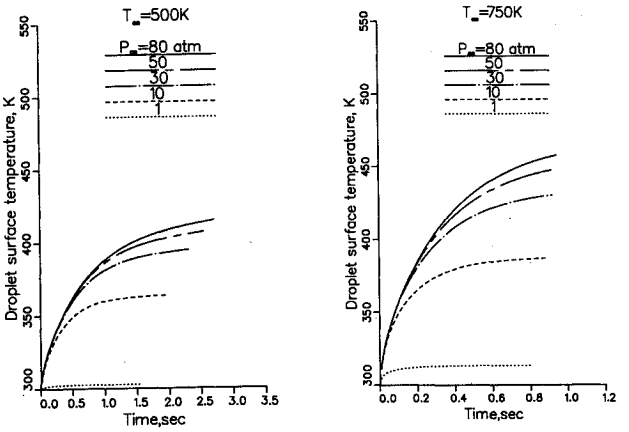

Fig. 4 Droplet surface temperature with time for different ambient pressures and temperatures.

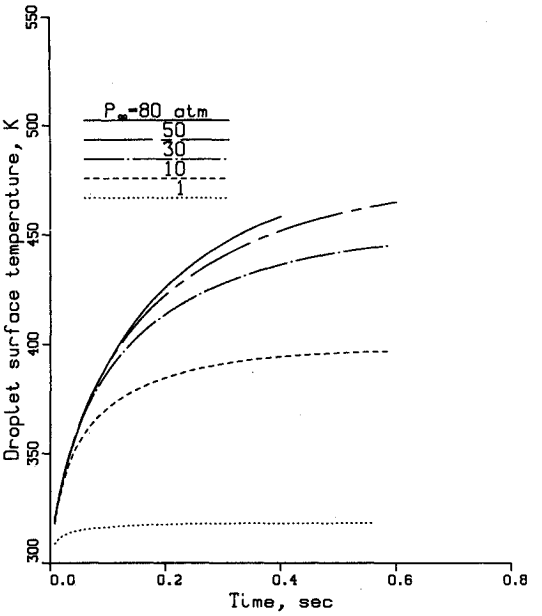

Fig. 5 Droplet surface temperature with time for different ambient pressures; $T_\infty = 1000$ K.

the droplet surface reaches a steady temperature, the so-called wet-bulb temperature. At supercritical pressures the droplet surface temperature keeps rising until the end of the droplet lifetime. Note that implementation of the limit presented in Fig. 2 can be seen in Fig. 5. Computation for the case corresponding to $P_\infty = 80$ atm was terminated early in the droplet lifetime; namely, at the moment the droplet surface temperature reached the highest acceptable equilibrium temperature (according to Fig. 2) at a total pressure of 80 atm. In view of this, computations for ambient pressures higher than 80 atm were not conducted for this particular ambient temperature. Upper limit in the ambient pressure was similarly established for the remaining ambient temperatures considered, and are reflected in Fig. 8, which is discussed later.

In Fig. 6 the final droplet surface temperature is plotted with total pressure for three different ambient temperatures (T_∞ = 500, 750, and 1000 K). The final temperatures are defined as the droplet surface temperatures at the end of the transient calculations which were terminated when $(R/R_0)^2 = 0.2$. It is shown that at low and moderate pressures, the final temperature increases with increasing pressures, and becomes almost independent of pressure at supercritical gaseous environments. However, it remains below the critical temperature of *n*-hexane, for the ambient temperatures and pressures considered (the critical temperature and pressure of *n*-hexane are 507.4 K and 29.3 atm, respectively). Kadota and Hiroyasu[18] experimentally predicted the same dependence of the final temperature with pressure for the burning of *n*-heptane droplets. In Fig. 7 the surface and center temperature of the droplet are presented with respect to time. During the initial period, the surface temperature changes rapidly, while the center temperature remains unchanged. At low pressures, the droplet reaches a uniform and constant temperature early in its lifetime, whereas at high pressures, a temperature gradient exists in the droplet interior for most of its lifetime.

Figure 8 shows the dimensionless droplet lifetime as a function of total pressure for five different ambient temperatures (T_∞ = 500, 600, 750, 1000, and 1250 K). The dimensionless droplet lifetime is given by $\tau\beta/D_0^2$, where τ is the dimensional droplet lifetime, D_0 is the initial droplet diameter, and β is the evaporation constant for a droplet evaporating while at its wet-bulb temperature, ambient pressure of 1 atm and ambient temperature is as indicated in Figs. 8 and 9 for each curve (β = 0.13, 0.18, 0.25, 0.36, and 0.47 mm^2/s for T_∞ = 500, 600, 750, 1000, and 1250 K, respectively). The heat transferred to the droplet surface from the gaseous phase is utilized for heating-up of the droplet interior and for evaporation of the liquid droplet. If the surface temperature is lower than the wet-bulb temperature, the heat-up consumes a significant portion of the energy transported to the surface. When the surface temperature reaches the wet-bulb temperature, most of the energy transferred to the surface is utilized for vaporization. Thus, the heating-up of the droplet interior prolongs the droplet lifetime. Since the wet-bulb temperature increases with ambient pressures, the droplet heat-up time, as compared to its lifetime, becomes more important at high pressures.[1] There is a second cause that may prolong the droplet lifetime. Figures 4 and 5 indicate that the temperature T_s at the droplet surface increases with increasing pressure, leading to a smaller temperature difference between T_∞ and T_s. Since this temperature difference is the driving force for heat transfer towards the droplet, the reduced temperature difference

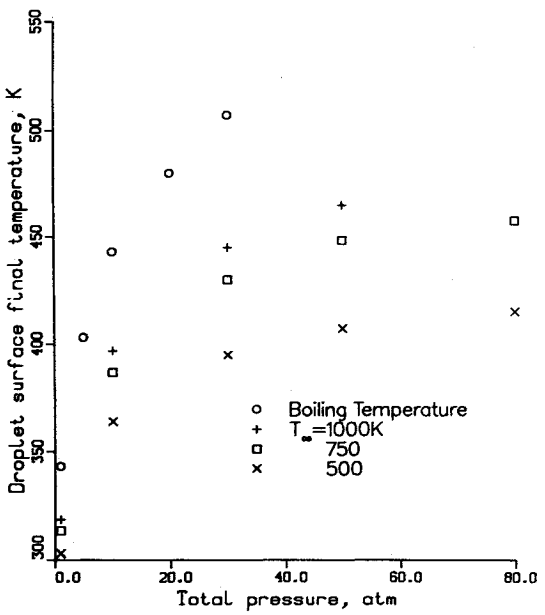

Fig. 6 Droplet surface final temperature with total pressure for different ambient temperatures.

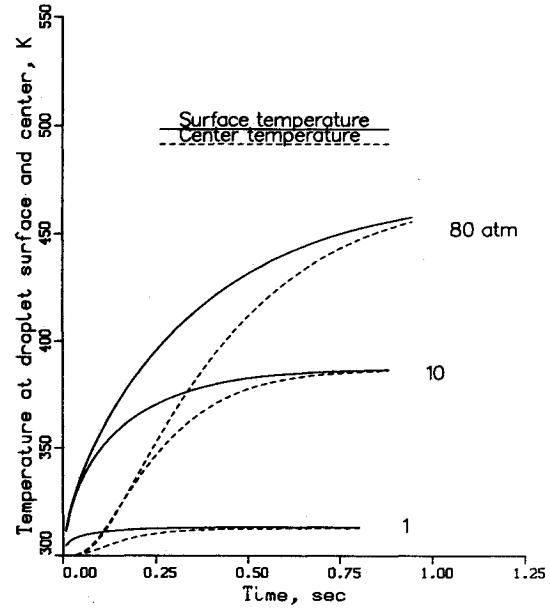

Fig. 7 Temporal variation of surface and center temperature of the droplet for different ambient pressures; T_∞ = 750 K.

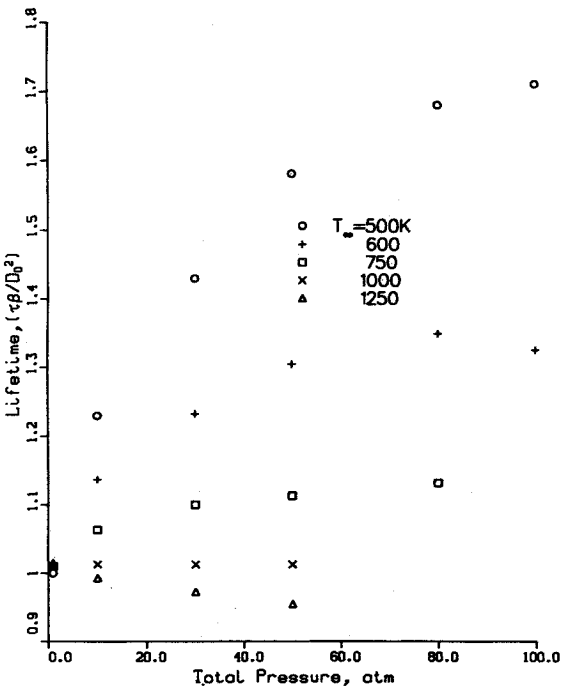

Fig. 8 Dimensionless droplet lifetime with total pressure for five different ambient temperatures.

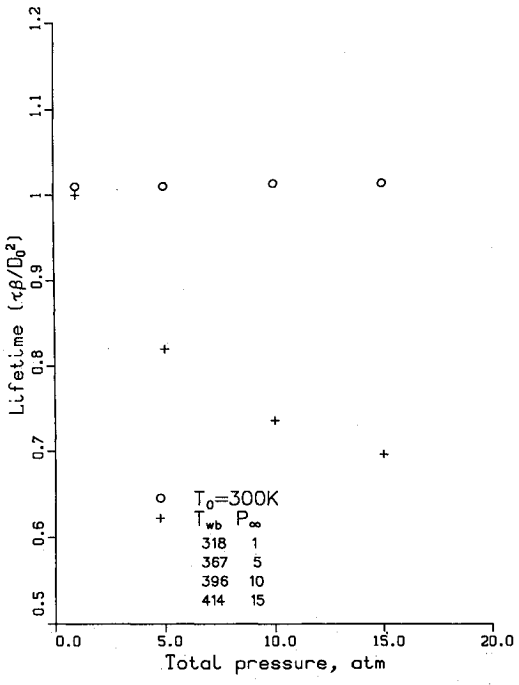

Fig. 9 Dimensionless droplet lifetime with total pressure (T_∞ = 1000 K); open circles: droplets initially at 300 K, crosses: droplets under steady state vaporization.

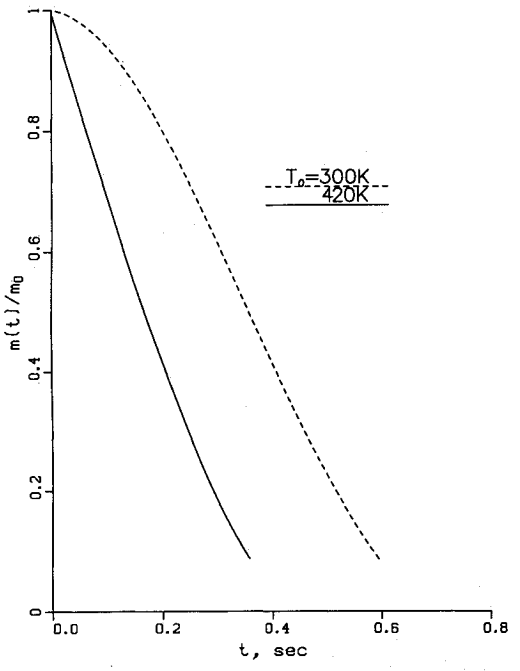

Fig. 10 Dimensionless droplet mass as a function of time for two different intial temperatures; T_∞ = 1000 K and P_∞ = 50 atm.

tends to prolong the droplet lifetime with increasing pressure. With respect to mass transfer away from the droplet surface (which, of course, is strongly coupled with the heat transfer problem) the tendency is to decrease with increasing ambient pressure for two reasons 1) the binary mass diffusion coefficient is inversely proportional to pressure; and 2) the equilibrium mole fraction of the vaporizing species at the droplet surface decreases with increasing pressure (see Fig. 2). The lower the mole fraction of the vapor at the droplet surface, the smaller its spatial gradient outside the droplet. Consequently, the mass transfer driving force weakens at higher ambient pressure, and therefore contributes in prolonging the droplet lifetime. However, as shown in Fig. 3, the energy required for phase change decreases with increaisng total pressure and equilibrium temperature. Since the higher the ambient pressure, the higher the equilibrium temperature, the energy required for vaporization is reduced with increasing total pressure, which tends to shorten the droplet lifetime. The competing mechanisms described above determine the length of the droplet lifetime. Thus, for the lowest ambient temperature (500 K) of Fig. 8, apparently the increase in the droplet heat-up and the reduction in the driving forces for heat and mass transfer, are more important than the reduction of the energy required for vaporization with increasing pressure, leading to increased droplet lifetime with increasing ambient pressure, at least for the pressure range considered. It appears highly probable that at pressures higher than those we were able to examine in the present study, the droplet lifetime might reach a maximum, and subsequently decrease with pressure. Such dependence of droplet lifetime on pressure is clealy shown for T_∞ = 600 K. At higher ambient temperatures the droplet lifetime is less sensitive to pressure (1000 K). For even higher ambient temperatures (1250 K), it decreases monotonically with ambient pressure. The monotonic decrease of droplet lifetime with pressure at high ambient temperatures was also predicted by Hsieh et al.[21] who conducted their calculations for a single ambient temperature of 2000 K. Of course, at a given ambient pressure, the droplet lifetime is reduced significantly with increasing ambient temperature.

The next two figures are relevant to the steady-state vaporization assumption. By steady state, it is implied that all the energy arriving at the droplet surface is utilized for vaporization, while the droplet remains at a constant temperature. Furthermore, the gas phase is considered quasisteady. Figure 9 shows the droplet lifetime for a range of low to moderate ambient pressures (1–15 atm). For this pressure range, as can be seen from Fig. 5, there is clearly a wet-bulb temperature, T_{wb}. In Fig. 9, the open circles were obtained using our complete numerical model, with the droplet initially at 300 K. These calculations provided the wet-bulb temperature corresponding to each of the ambient pressures considered. Using quasisteady gas phase while the droplet temperature remains constant at its wet bulb value, the steady-state assumption as defined above and used by Manrique and Borman[6] was employed. The predictions are indicated by crosses in Fig. 9. As can be seen, the droplet lifetime is decreasing steeply with ambient pressure. At very low pressure (1 atm) the steady-state assumption is valid, mainly since there is very little heat-up of the droplet interior. However, even at the moderate pressure of 15 atm, the droplet lifetime is substantially underpredicted, indicating that the heat-up becomes very important with increasing pressure. This can be seen more clearly in Fig. 10 where the dimensionless droplet mass is plotted for two different initial temperatures (T_0 = 300 and 420 K). Choosing T_0 = 420 K almost eliminates the heat-up. There is still heat-up of the droplet interior, since as was mentioned earlier in the discussion of Figs. 4 and 5, at very high ambient pressures, the droplet surface temperature keeps increasing until the end of the droplet lifetime. The smaller slope of the dashed curve during the early part of the droplet lifetime, clearly shows that at high ambient pressure, droplet heat-up time is very important in comparison to droplet lifetime.

C. Conclusions

For low and intermediate ambient pressures a wet-bulb temperature is predicted, however, at supercritical pressures the droplet surface temperature keeps rising until the end of the droplet lifetime. For the range of pressures considered, it is predicted that droplet surface temperatures level off below the critical temperature of the droplet.

The droplet lifetime dependence on ambient pressure and temperature is quite complex. At the low ambient temperature of 500 K, for the pressure range considered (1–100 atm), the droplet lifetime increases with increasing ambient pres-

sure, at 600 K, the droplet lifetime presents a maximum. At higher ambient temperatures, the droplet lifetime is less sensitive to pressure (1000 K), and decreases monotonically with pressure at even higher temperatures (1250 K). The competing mechanisms that define the droplet lifetime behavior have been clearly delineated.

The steady-state vaporization assumption fails severely with increasing ambient pressure and underpredicts droplet lifetime substantially.

The major assumption in this study has been the impermeability condition. At high ambient pressure the inert gas dissolves into the liquid phase. The numerical model of Hsieh et al.[21] includes solubility effects by considering all species in thermodynamic equilibrium in both phases. Such treatment removes the limitations imposed on the ambient pressures and temperatures (Fig. 2) that can be investigated. However, for the range of pressures and temperatures considered in the present study, the effect of solubility is not so important to significantly alter the results presented. Hsieh et al.[10] have shown that even up to ambient pressures as high as 70 atm, the mass fraction of the dissolved nitrogen in a two-component (*n*-pentane and *n*-octane) liquid droplet remains below 0.06.

Acknowledgments

The authors are very grateful for the support of this research by the Rutgers University Research Council Program and by the Department of Mechanical and Aerospace Engineering. Computational work was performed on the Supercomputer Remote Access and Graphics Center at Rutgers University and the Pittsburgh Supercomputing Center. The support of both computing facilities is greatly appreciated.

References

[1]Faeth, G. M., "Current Status of Droplet and Liquid Combustion," *Progress in Energy and Combustion Science*, Vol. 3, No. 3, 1977, pp. 191–224.

[2]Law, C. K., "Recent Advances in Droplet Vaporization and Combustion," *Progress in Energy and Combustion Science*, Vol. 8, No. 3, 1982, pp. 171–201.

[3]Sirignano, W. A., "Fuel Droplet Vaporization and Spray Combustion Theory," *Progress Energy and Combustion Science*, Vol. 9, No. 4, 1983, pp. 291–322.

[4]Williams, F. A., *Combustion Theory*, 2nd ed., Benjamin/Cummings Publishing, Menlo Park, CA, 1985, pp. 52–69.

[5]Matlosz, R. L., Leipziger, S., and Torda, T. P., "Investigation of Liquid Drop Evaporation in a High Temperature and High Pressure Environment," *International Journal of Heat and Mass Transfer*, Vol. 15, No. 4, 1972, pp. 831–852.

[6]Manrique, J. A., and Borman, G. L., "Calculations of Steady State Droplet Vaporization at High Ambient Pressures," *International Journal of Heat and Mass Transfer*, Vol. 12, No. 9, 1969, pp. 1081–1095.

[7]Hubbard, G. L., Denny, V. E., and Mills, A. E., "Droplet Evaporation: Effects of Transients and Variable Properties," *International Journal of Heat and Mass Transfer*, Vol. 18, No. 9, 1975, pp. 1003–1008.

[8]Curtis, E. W., and Farrell, P. V., "Droplet Vaporization in a Supercritical Microgravity Environment," *Acta Astronautica*, Vol. 17, Nos. 11 and 12, 1988, pp. 1189–1193.

[9]Curtis, E. W., Hartfield, J. P., and Farrell, P. V., "Microgravity Vaporization of Liquid Droplets under Supercritical Conditions," *Proceedings of Third Colloquium on Drops and Bubbles*, American Inst. of Physics, Monterey, CA, 1988, pp. 373–386.

[10]Hsieh, K. C., Shuen, J. S., and Yang, V., "Analysis of Multi-Component Droplet Vaporization at Near Critical Conditions," AIAA 26th Aerospace Sciences Meeting, AIAA Paper 88-0637, Reno, NV, Jan. 1988.

[11]Delplanque, J. P., and Sirignano, W. A., "Transient Vaporization and Burning for an Oxygen Droplet at Sub- and Near-Critical Conditions," AIAA 29th Aerospace Sciences Meeting, AIAA Paper 91-0075, Reno, NV, Jan. 1991.

[12]Hall, A. R., and Diederichsen, J., "An Experimental Study of the Burning of Single Drops of Fuel in Air at Pressure up to Twenty Atmospheres," *Fourth (International) Symposium on Combustion*, Combustion Inst., Pittsburgh, Vol. 4, 1953, pp. 837–846.

[13]Rosner, D. E., "On Liquid Droplet Combustion at High Pressure," *AIAA Journal*, Vol. 5, No. 1, 1967, pp. 163–166.

[14]Faeth, G. M., Dominicis, D. P., Tulpinsky, J. F., and Olson, D. R., "Supercritical Bipropellant Droplet Combustion," *Twelfth (International) Symposium on Combustion*, Combustion Inst., Pittsburgh, PA, Vol. 12, 1969, pp. 9–18.

[15]Lazar, Q. S., and Faeth, G. M., "Bipropellant Droplet Combustion in the Vicinity of the Critical Point," *Thirteenth (International) Symposium on Combustion*, Combustion Inst., Pittsburgh, PA, Vol. 13, 1971, pp. 743–753.

[16]Rosner, D. E., and Chang, W. S., "Transient Evaporation and Combustion of a Fuel Droplet near its Critical Temperature," *Combustion Science and Technology*, Vol. 7, No. 4, 1973, pp. 145–158.

[17]Canada, G. S., and Faeth, G. M., "Fuel Droplet Burning Rates at High Pressures," *Fourteenth (International) Symposium on Combustion*, Combustion Inst., Pittsburgh, PA, Vol. 13, 1973, pp. 1345–1354.

[18]Kadota, T., and Hiroyasu, H., "Combustion of a Fuel Droplet in Supercritical Gaseous Environments," *Eighteenth (International) Symposium on Combustion*, Combustion Inst., Pittsburgh, PA, Vol. 18, 1981, pp. 275–282.

[19]Shuen, J. S., and Yang, V., "Combustion of Liquid-Fuel Droplets in Supercritical Conditions," AIAA 29th Aerospace Sciences Meeting, AIAA Paper 91-0078, Reno, NV, Jan. 1991.

[20]Sato, J. I., Tsue, M., Niwa, M., and Kono, M., "Effects of Natural Convection on High-Pressure Droplet Combustion," *Combustion and Flame*, Vol. 82, No. 2, 1990, pp. 142–150.

[21]Hsieh, K. C., Shuen, J. S., and Yang, V., "Droplet Vaporization in High-Pressure Environments I: Near Critical Conditions," *Combustion Science and Technology*, Vol 76, Nos. 1–3, 1991, pp. 111–132.

[22]McCreath, C. G., and Chigier, N. A., "Liquid Spray Burning in the Wake of Stabilizer Disc," *Fourteenth (International) Symposium on Combustion*, Combustion Inst., Pittsburgh, PA, Vol. 14, 1972, pp. 1355–1363.

[23]Chigier, N. A., and McCreath, C. G., "Combustion of Droplets in Sprays," *Acta Astronautica*, Vol. 1, Nos. 4 and 5, 1974, pp. 687–709.

[24]Khalil, E. E., and Whitelaw, J. H., "Aerodynamics Characteristics of Kerosene-Spray Flames," *Sixteenth (International) Symposium on Combustion*, Combustion Inst., Pittsburgh, PA, Vol. 16, 1976, pp. 569–576.

[25]Onuma, Y., and Ogasawara, M., "Studies on the Structure of a Spray Combustion Flame," *Fifteenth (International) Symposium on Combustion*, Combustion Inst., Pittsburgh, PA, Vol. 15, 1974, pp. 453–465.

[26]Kawazoe, H., Ohsawa, K., and Fujikake, K., "LDA Measurement of Fuel Droplet Sizes and Velocities in the Combustion Field," *Combustion and Flame*, Vol. 82, No. 2, 1990, pp. 151–162.

[27]Chueh, P. L., and Prausnitz, J. M., "Vapor-Liquid Equilibria at High Pressure: Vapor-Phase Fugacity Coefficients in Nonpolar and Quantum-Gas Mixtures," *Industrial and Engineering Chemistry Fundamentals*, Vol. 6, No. 4, 1967, pp. 492–498.

[28]Reid, R. C., Prausnitz, J. M., and Polling, B. E., *The Properties of Gases and Liquids*, 4th ed., McGraw-Hill, New York, 1987, pp. 388–631.

[29]Neufeld, P. D., Janzen, A. R., and Aziz, R. A., "Empirical Equations to Calculate 16 of the Transport Collision Integrals $\Omega^{(l,s)}$ for the Lennard-Jones Potential," *Journal of Chemical Physics*, Vol. 57, No. 3, 1972, pp. 1100–1102.

[30]Roy, G., and Thodos, D., "Thermal Conductivity of Gases—Organic Compounds at Atmospheric Pressure," *Industrial and Engineering Chemistry Fundamentals*, Vol. 9, No. 1, 1970, pp. 71–79.

[31]Stiel, L. I., and Thodos, G., "The Thermal Conductivity of Nonpolar Substances in the Dense Gaseous and Liquid Regions," *American Institute of Chemical Engineers Journal*, Vol. 10, No. 1, 1964, pp. 26–30.

[32]Prausnitz, J. M., and Gunn, R. D., "Volumetric Properties of Nonpolar Gaseous Mixtures," *American Institute of Chemical Engineers Journal*, Vol. 4, No. 4, 1958, pp. 430–494.

[33]Takahashi, S., "Preparation of a Generalized Chart for the Diffusion Coefficients of Gases at High Pressure," *J. Chem. Eng. Japan*, Vol. 6, No. 6, 1974, pp. 417–420.

[34]Patankar, S. V., "Numerical Heat Transfer and Fluid Flow," 1st ed., Hemisphere, New York, 1980, pp. 56–58.

[35]Poston, R. R., and McKetta, J. J., "Vapor-Liquid Equilibrium in the N-Hexane-Nitrogen System," *Journal of Chemical and Engineering Data*, Vol. 11, No. 3, 1966, pp. 364–365.